1. Introduction

Many studies have reported the prognostic significance of nodal metastasis and have emphasized that the number of nodal metastases is the most significant prognostic parameter in predicting the outcome of patients with invasive ductal carcinoma with nodal metastasis [1-5]. Among other parameters associated with nodal metastasis, the presence of extranodal invasion or the dimensions of the nodal metastases have been reported to be important prognostic parameters [1-10]. We previously examine which factors of metastatic mammary carcinoma to the lymph nodes were significantly associated with the outcome of patients with invasive ductal carcinoma and clearly demonstrated that the number of mitotic figures in metastatic mammary carcinoma to the lymph nodes was the most important factor for accurately predicting the outcome of patients with invasive ductal carcinoma with nodal metastasis [11].

To confirm these previous findings, the present study investigated the number of mitotic figures in metastatic mammary carcinoma to the lymph nodes and other histologic characteristics of metastatic mammary carcinoma to the lymph nodes known to be significantly associated with patient outcome according to nodal status in a different patient series of patients with invasive ductal carcinoma of the breast. We confirmed that the number of mitotic figures in metastatic mammary carcinoma to the lymph nodes was a very important outcome predictive factor for patients with invasive ductal carcinoma independent of the nodal status and the histologic grade of the primary invasive ductal carcinoma.

2. Materials and methods

2.1. Cases

The subjects of this study were 1039 consecutive patients with invasive ductal carcinoma of the breast who did not receive neoadjuvant therapy and were surgically treated at the National Cancer Center Hospital between January 2000 and December 2005. The invasive ductal carcinomas were diagnosed preoperatively using a needle biopsy, aspiration cytology, mammography, or ultrasonography. All the patients were Japanese women, ranging in age from 23 to 72 years (median, 55 years). All the patients had a solitary lesion; 495 patients were premenopausal, and 544 were postmenopausal. A partial mastectomy had been performed in 456 patients, and a modified radical mastectomy had been performed in 583 patients. A level I and a level II axillary lymph node dissection had been performed in all the patients, and a level III axillary lymph node dissection had been performed in some of the patients.

Of the 1039 patients, 870 received adjuvant therapy, consisting of chemotherapy in 217 patients, endocrine therapy in 280 patients, and chemoendocrine therapy in 373 patients. The chemotherapy regimens were either anthracycline based with or without taxane or non–anthracycline based. The endocrine therapy regimens consisted of tamoxifen with or without a gonadotropin-releasing hormone agonist, tamoxifen with or without an aromatase inhibitor, an aromatase inhibitor alone, or a gonadotropin-releasing hormone agonist alone. No cases of inflammatory breast cancer were included in this series. All the tumors were classified according to the present Union Internationale Contre le Cancer pTNM classification [12]. The protocol for this study (20-112) was reviewed by the Institutional Review Board of the National Cancer Center.

For the pathologic examination, the surgically resected specimens were fixed in 10% formalin; and the size and gross appearance of the tumors were recorded. The tumor size was confirmed by comparison with the tumor size on the histologic slides.

2.2. Histologic examination

Serial sections of each primary tumor area were cut from paraffin blocks. One section from each tumor was stained with hematoxylin and eosin and was examined histologically to confirm the diagnosis; the other sections were used for immunohistochemistry. The following 10 histologic factors of the primary invasive ductal carcinomas were evaluated: (1) invasive tumor size (≤20 mm, >20 to ≤50 mm, >50 mm), (2) histologic grade (1, 2, and 3) [13], (3) number of mitotic figures in the primary invasive ductal carcinoma (≤5 and >5), (4) tumor necrosis (absent or present) [14], (5) fibrotic focus (absent, fibrotic focus diameter ≤8 mm, fibrotic focus diameter >8 mm) [15,16], (6) grading system for lymph vessel tumor emboli [17,18], (7) blood vessel invasion (absent or present), (8) adipose tissue invasion (absent or present), (9) skin invasion (absent or present), and (10) muscle invasion (absent or present).

The nodal metastases were evaluated using single sections of each node or half of each node stained with hematoxylin and eosin. The nodal metastases were not examined immunohistochemically in this study. The 9 histologic parameters of metastatic mammary carcinoma to the lymph nodes listed in Table 1 were examined [11]. We randomly searched for mitotic figures in metastatic mammary carcinoma to the lymph nodes using midpower magnification fields (×10 or ×20) of the tumor area and selected 1 high-power magnification field (×40) of the tumor area with the highest number of mitotic figures in metastatic mammary carcinoma to the lymph nodes to determine the largest number of metastatic mammary carcinoma to the lymph nodes exhibiting mitotic figures (Fig. 1) [11]. In the primary invasive ductal carcinoma, the presence of 6 or more mitotic figures in 1 high-power magnification field

Table 1 Histologic factors of metastatic mammary carcinoma to the lymph nodes

Factors
No. of nodal metastases
No nodal metastasis
1-3 nodal metastases
4-9 nodal metastases
≥10 nodal metastases
Maximum dimension of metastatic mammary carcinoma to the lymph nodes (mm)
No nodal metastasis
≤20
>20
Histologic grade
No nodal metastasis
Grade 1
Grade 2
Grade 3
No. of mitotic figures in metastatic mammary carcinoma cells visible in 1 high-power magnification field
No nodal metastasis
≤5
>5
Fibrotic focus
No nodal metastasis
Absent
Present
Tumor necrosis
No nodal metastasis
Absent
Present
Grade of stromal fibrosis in metastatic mammary carcinoma to the lymph nodes
No nodal metastasis
None
Mild
Moderate
Severe
No. of lymph nodes with extranodal invasion
No nodal metastasis
≤5
>5
No. of extranodal blood vessel tumor emboli
No nodal metastasis
≤9
>9

was assessed in the same manner as for metastatic mammary carcinoma to the lymph nodes to enable a direct comparison. The histologic grade and presence of tumor necrosis in metastatic mammary carcinoma to the lymph nodes were evaluated in the same manner as for the primary invasive ductal carcinomas.

Immunohistochemical staining for estrogen receptors, progesterone receptors, p53, and HER2 products in the primary invasive ductal carcinoma was performed using an autoimmunostainer (Optimax Plus; BioGenex, San Ramon, CA). The antigen retrieval device for the Optimax Plus was an autoclave, and each specimen was immersed in citrate buffer and incubated at 121°C for 10 minutes. Immunoperoxidase staining was performed using a labeled streptavidin-biotin staining kit (BioGenex) according to the manufacturer's instructions. The antibodies that were used were antiestrogen receptor mouse monoclonal antibody ER88 (BioGenex), antiprogesterone receptor mouse monoclonal antibody PR88 (BioGenex), anti-HER2 mouse monoclonal antibody CB11 (BioGnex), and p53 mouse monoclonal antibody DO7 (Dako, Glostrup, Denmark). ER88, PR88, and CB11 were previously diluted, and DO7 was applied at a dilution of 1:100. After immunostaining, the sections were counterstained with hematoxylin. Sections of the invasive ductal carcinomas that were positive for estrogen receptor, progesterone receptor, HER2, and p53 were used each time as a positive control. As a negative control, the primary antibody was replaced with normal mouse immunoglobulin.

Slides of primary invasive ductal carcinomas immunostained for estrogen receptor, progesterone receptor, and p53 were scored using the Allred scoring system, as described previously [19-21]. Briefly, each entire slide was evaluated using light microscopy. First, the proportion of positively stained tumor cells was estimated (0, none; 1, <1/100; 2, 1/100 to <1/10; 3, 1/10 to <1/3; 4, 1/3 to 2/3; and 5, >2/3). Next, the average intensity of positively stained tumor cells was estimated (0, none; 1, weak; 2, intermediate; and 3, strong). The proportion and intensity scores were then added to obtain the total score, which ranged from 0 or 2 to 8. The Allred scores for estrogen receptor, progesterone receptor, and p53 expression in the primary invasive ductal carcinomas were then classified into the following 3 categories [22]: (1) Allred score for estrogen receptor (0 or 2, 3-6, and 7 or 8); (2) Allred score for progesterone receptor (0 or 2, 3-6, and 7 or 8); and (3) Allred score for p53 (0 or 2 or 3, 4-6, and 7 or 8). The Allred score risk classification for p53 in primary

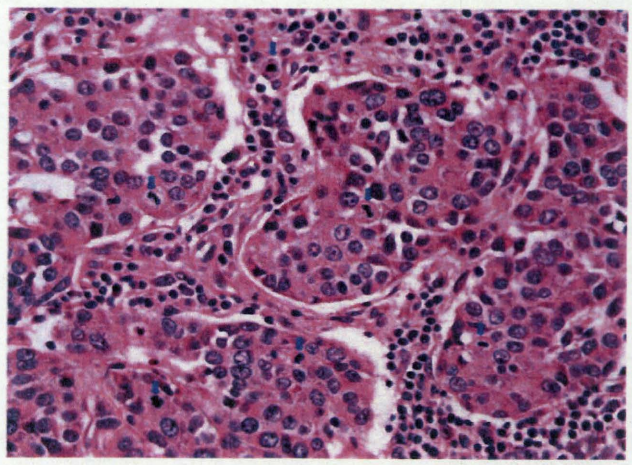

Fig. 1 Histologic features of metastatic mammary carcinoma to the lymph nodes. Six mitotic figures are visible in the tumor cells (arrows).

tumor-stromal fibroblasts forming and not forming fibrotic foci has been described in our previous study [23]. As the distribution of tumor-stromal fibroblasts expressing p53 is scattered, even in primary invasive ductal carcinomas with tumor-stromal fibroblasts with Allred scores of 4 to 8, we modified the Allred scoring system to assess the expression of p53 in tumor-stromal fibroblasts as follows. First, we scanned the entire tumor section stained for p53 at medium power (objective ×10 and ocular ×10) to identify the region with the highest proportion and intensity scores for p53 expression (ie, a "hot spot"), then the highest intensity score (0, none; 1, weak; 2, intermediate; 3, strong), not the average intensity score as in the original methodology, and the highest proportion score (0-5) for the expression of p53 were evaluated using 1 high-power field (hot spot, objective ×40 and ocular ×10). The proportion and intensity scores for the tumor-stromal fibroblasts were then added to obtain the total score, which ranged from 0 or 2 to 8. Finally, we devised an Allred score risk classification for p53 in tumor-stromal fibroblasts in invasive ductal carcinomas based on the combined Allred scores for p53 in tumor-stromal fibroblasts forming and not forming fibrotic foci (Table 2). The HER2 status of the primary invasive ductal carcinomas was semiquantitatively scored using a scale of 0 to 3 according to the level of HER2 protein expression [24] and was classified into 3 categories: 0 or 1, 2, or 3.

Table 2 Overall Allred score classification of p53 in tumor-stromal fibroblasts forming and not forming a fibrotic focus in primary invasive ductal carcinomas

Primary invasive ductal carcinoma with a fibrotic focus	Score class
Allred scores of p53 in tumor-stromal fibroblasts forming a fibrotic focus	
0, 2, or 3	0
4-8	2
Allred scores of p53 in tumor-stromal fibroblasts not forming a fibrotic focus	
0 or 2	0
3	1
4-8	2
Total (A + B)	0-4
Primary invasive ductal carcinoma without a fibrotic focus	Score class
Allred scores of p53 in tumor-stromal fibroblasts not forming a fibrotic focus	
0 or 2	0
3	1
4-8	2
Total	0-2
Allred score risk classes for p53 in tumor-stromal fibroblasts forming and not forming fibrotic foci in primary invasive ductal carcinomas	
Low-risk class	0 and 1
Intermediate-risk class	2 and 3
High-risk class	4

2.3. Patient outcome and statistical analysis

Survival was evaluated using a median follow-up period of 78 months (range, 32-116 months) until April 2010. Of the 1039 patients with invasive ductal carcinoma, 865 patients were alive and well, 174 had developed tumor recurrences, and 81 had died of their disease at the end of the study period. The tumor recurrence-free survival and overall survival periods were calculated using the time of surgery as the starting point. Tumor relapse was considered to have

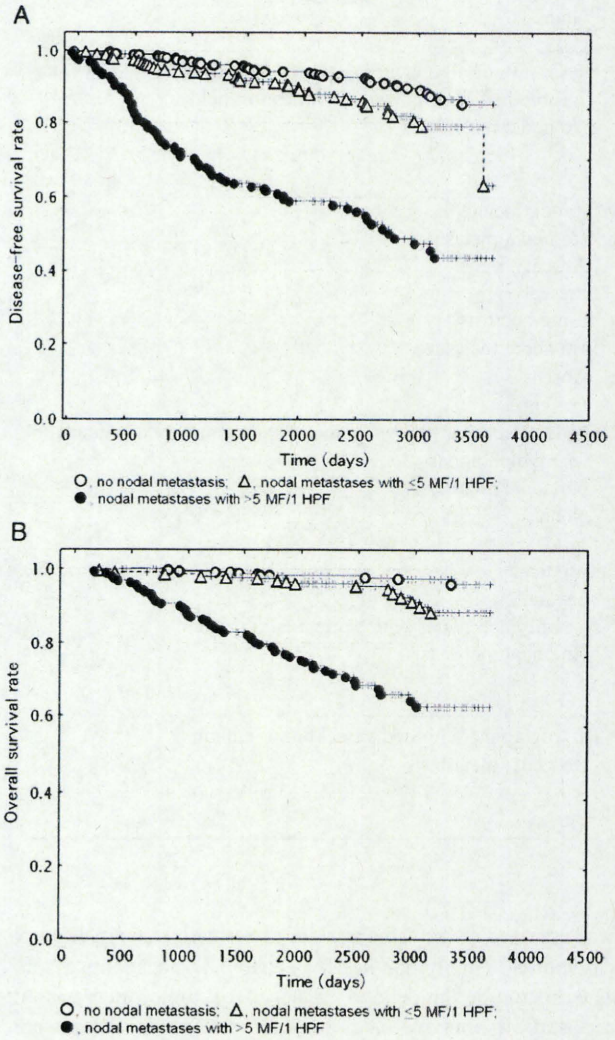

Fig. 2 A and B, Disease-free survival curves and overall survival curves of invasive ductal carcinoma patients according to the number of mitotic figures in metastatic mammary carcinoma to the lymph nodes. Both survival curves decreased significantly according to the number of mitotic figures in metastatic mammary carcinoma to the lymph nodes.

occurred whenever evidence of distant organ metastasis or local recurrence was found.

We analyzed the outcome predictive power of the histologic factors of the primary invasive ductal carcinomas and metastatic mammary carcinoma to the lymph nodes, the immunohistochemical findings, the use of adjuvant therapy (yes or no), and the patient age (≤39 and >39 years) according to the nodal status or the histologic grade of the

Table 3 Multivariate analyses for tumor recurrence and tumor-related death in patients with invasive ductal carcinoma patients overall

	Cases	Tumor recurrence			Tumor-related death		
		Cases (%)	HR, 95% CI	*P*	Cases (%)	HR, 95% CI	*P*
No. of mitotic figures in metastatic mammary carcinoma to the lymph nodes							
No	591	52 (9)	1		13 (2)	1	
<5	283	43 (15)	1		17 (6)	1	
>5	165	79 (48)	2.3 1.5-3.7	<.001	51 (31)	2.3 1.2-4.3	.012
Allred scores for progesterone receptors in primary invasive ductal carcinoma cells							
0 or 2	183	45 (25)	1		23 (13)	1	
3-6	302	59 (20)	0.7 0.5-1.1	.164	35 (12)	0.9 0.5-1.7	.776
7 or 8	554	70 (13)	0.6 0.4-0.9	.020	23 (4)	0.4 0.2-0.7	<.001
Blood vessel invasion							
Absent	890	131 (15)	1		55 (6)	1	
Present	149	43 (29)	1.6 1.1-2.4	.021	26 (18)	1.8 1.1-3.0	.023
Fibrotic focus, diameter (mm), in primary invasive ductal carcinomas							
Absent	664	85 (13)	1		35 (5)	1	
<8	221	37 (17)	1.4 0.8-2.4	.157	14 (6)	1.7 0.8-3.6	.209
>8	154	52 (34)	2.2 1.4-3.5	.001	32 (40)	2.1 1.3-3.6	.004
Grading system for lymph vessel tumor emboli							
Grade 0	664	71 (11)	1		28 (4)	1	
Grade 1	249	39 (16)	1.3 0.8-1.9	.282	15 (6)	1.3 0.7-2.6	.389
Grade 2	97	43 (44)	2.4 1.5-3.8	<.001	22 (23)	2.1 1.2-3.6	.011
Grade 3	29	21 (72)	3.8 2.0-7.2	<.001	16 (55)	2.3 1.2-4.5	.014
Histologic grade of metastatic mammary carcinoma to the lymph nodes							
No	591	52 (9)	1		13 (2)	1	
Grade 1	98	7 (7)	1		1 (1)	1	
Grade 2	172	46 (27)	1.2 0.7-2.0	.638	20 (12)	3.6 1.6-8.0	.002
Grade 3	177	69 (39)	2.0 1.2-3.1	.004	47 (27)	3.9 1.6-9.2	.002
Histologic grade of primary invasive ductal carcinomas							
Grade 1	260	14 (5)	1		1 (0.4)	1	
Grade 2	438	57 (13)	1.6 0.9-3.0	.107	24 (6)	6.4 0.8-48.6	.075
Grade 3	341	103 (30)	2.0 1.0-3.8	.034	56 (16)	8.5 1.1-63.6	.039
p53 Allred score risk classes of tumor-stromal fibroblasts forming and not forming a fibrotic focus in primary invasive ductal carcinomas							
Low	714	69 (10)	1		19 (3)	1	
Inter	263	76 (30)	2.3 1.6-3.3	<.001	42 (16)	3.7 2.1-6.5	<.001
High	46	25 (54)	3.0 1.7-5.3	<.001	17 (37)	4.3 2.1-9.1	<.001

Abbreviations: HR indicates hazard rate; CI, confidence interval; Low, low risk; Inter, intermediate risk; High, high risk.

primary invasive ductal carcinomas for tumor recurrence and tumor-related death using univariate analyses with the Cox proportional hazards regression model. The factors significantly associated with outcome in the univariate analyses were then used in a multivariate analysis using the Cox proportional hazards regression model. The case-wise and step-down method was applied until all the remaining factors were significant at a P value of less than .05. All the analyses were performed using Statistica/Windows software (StatSoft, Tulsa, OK).

3. Results

3.1. Factors significantly associated with patient outcome

Overall, the presence of 6 or more mitotic figures in metastatic mammary carcinoma to the lymph nodes (Fig. 2A and B), blood vessel invasion, a fibrotic foci with a diameter greater than 8 mm in the primary invasive ductal carcinoma, grade 2 or 3 lymph vessel tumor emboli, histologic grade 3 metastatic mammary carcinoma to the lymph nodes, histologic grade 3 primary invasive ductal carcinoma, and intermediate- and high-risk classes for p53 in tumor-stromal fibroblasts forming and not forming a fibrotic focus in the primary invasive ductal carcinomas significantly increased the hazard ratios for tumor recurrence and tumor-related death in the multivariate analyses (Table 3). An Allred score of 7 or 8 for progesterone receptors in the primary invasive ductal carcinoma significantly decreased the hazard ratios for tumor recurrence and tumor-related death in the multivariate analyses (Table 3). Histologic grade 2 metastatic mammary carcinoma to the lymph nodes significantly increased the hazard ratio for tumor-related death in the multivariate analyses (Table 3).

Among the patients with invasive ductal carcinoma with nodal metastasis, the presence of 6 or more mitotic figures in metastatic mammary carcinoma to the lymph nodes, blood vessel invasion, grade 2 or 3 lymph vessel tumor emboli, and intermediate- and high-risk classes for p53 in tumor-stromal fibroblasts forming and not forming a fibrotic focus in the primary invasive ductal carcinomas significantly increased

Table 4 Multivariate analyses for tumor recurrence and tumor-related death in patients with invasive ductal carcinoma with nodal metastases

	Cases	Tumor recurrence			Tumor-related death		
		Cases (%)	HR, 95% CI	P	Cases (%)	HR, 95% CI	P
No. of mitotic figures in metastatic mammary carcinoma to the lymph nodes							
<5	283	43 (15)	1		17 (6)	1	
>5	165	79 (48)	2.6 1.7-3.8	<.001	51 (31)	2.8 1.4-5.7	.004
Allred scores for progesterone receptors in primary invasive ductal carcinoma cells							
0 or 2	79	30 (38)	1		17 (22)	1	
3-6	133	41 (31)	0.7 0.4-1.2	.151	30 (23)	0.8 0.4-1.7	.581
7 or 8	236	51 (21)	0.6 0.3-0.9	.040	21 (9)	0.4 0.2-0.8	.019
Blood vessel invasion							
Absent	360	86 (24)	1		44 (12)	1	
Present	87	36 (41)	1.8 1.2-2.7	.007	24 (28)	2.0 1.1-3.8	.029
Grading system for lymph vessel tumor emboli							
Grade 0	199	34 (17)	1		18 (9)	1	
Grade 1	138	31 (23)	1.3 0.8-2.2	.306	13 (9)	1.3 0.6-2.9	.448
Grade 2	83	37 (45)	2.3 1.5-3.4	<.001	22 (27)	2.2 1.1-4.3	.030
Grade 3	28	20 (71)	2.8 1.6-4.8	<.001	15 (53)	2.9 1.3-6.1	.007
p53 Allred score risk classes of tumor-stromal fibroblasts forming and not forming a fibrotic focus in primary invasive ductal carcinomas							
Low	300	50 (17)	1		18 (6)	1	
Inter	115	51 (44)	2.1 1.4-3.2	<.001	33 (29)	2.9 1.5-5.7	.001
High	28	20 (71)	2.8 1.5-5.0	<.001	16 (57)	4.5 1.8-11.3	.001

the hazard ratios for tumor recurrence and tumor-related death in the multivariate analyses (Table 4). The Allred score of 7 or 8 for progesterone receptors in the primary invasive tumor cells significantly decreased the hazard ratios for tumor recurrence and tumor-related death in the multivariate analyses (Table 4).

Among the patients with histologic grade 1 primary invasive ductal carcinoma, the presence of 6 or more mitotic figures in metastatic mammary carcinoma to the lymph nodes ($P = .006$), lymph vessel tumor emboli grades 1 ($P = .007$) and 2 ($P = .009$), and a high-risk class for p53 in tumor-stromal fibroblasts forming and not forming a fibrotic focus in the primary invasive ductal carcinoma ($P = .015$) significantly increased the hazard ratios for tumor recurrence in the multivariate analyses. Because only 1 patient died because of her disease in this patient series, a multivariate analysis for tumor-related death could not be performed.

Among the patients with histologic grade 2 primary invasive ductal carcinoma, the presence of 6 or more mitotic figures in metastatic mammary carcinoma to the lymph nodes, a fibrotic foci with a diameter greater than 8 mm in the primary invasive ductal carcinoma, grade 2 or 3 lymph vessel tumor emboli, and intermediate- and high-risk classes for p53 in tumor-stromal fibroblasts forming and not forming a fibrotic focus in the primary invasive ductal carcinoma significantly increased the hazard ratios for tumor recurrence and tumor-related death in the multivariate analyses (Table 5). An Allred score of 3 or more for estrogen receptors in the primary invasive ductal carcinoma significantly decreased the hazard ratio for tumor recurrence and tumor-related death in the multivariate analyses (Table 5).

Among the patients with histologic grade 3 primary invasive ductal carcinoma, the presence of 6 or more mitotic figures in metastatic mammary carcinoma to the lymph nodes, blood vessel invasion, a fibrotic foci with a diameter greater than 8 mm in the primary invasive ductal carcinoma, grade 2 or 3 lymph vessel tumor emboli, and intermediate- and high-risk classes for p53 in tumor-stromal fibroblasts forming and not forming a fibrotic focus in the primary invasive ductal carcinoma significantly increased the hazard ratios for tumor recurrence and tumor-related death in the multivariate analyses (Table 6). The presence of 9 or more extranodal blood vessel tumor emboli significantly

Table 5 Multivariate analyses for tumor recurrence and tumor-related death in patients with histologic grade 2 invasive ductal carcinoma

	Cases	Tumor recurrence			Tumor-related death		
		Cases (%)	HR, 95% CI	*P*	Cases (%)	HR, 95% CI	*P*
No. of mitotic figures in metastatic mammary carcinoma to the lymph nodes							
No	251	19 (8)	1		3 (1)	1	
<5	149	20 (13)	1		9 (6)	1	
>5	38	18 (47)	3.1 1.6-5.9	<.001	12 (32)	5.4 2.1-13.5	<.001
Allred scores for estrogen receptors in primary invasive ductal carcinoma cells							
0 or 2	56	15 (27)	1		11 (20)	1	
3-6	57	5 (9)	0.3 0.1-0.8	.015	2 (4)	0.1 0.02-0.7	.022
7 or 8	325	37 (11)	0.4 0.2-0.7	.002	11 (3)	0.2 0.07-0.5	.001
Fibrotic focus, diameter (mm), in primary invasive ductal carcinomas							
Absent	283	26 (9)	1		10 (3)	1	
<8	99	14 (14)	1.5 0.7-2.9	.260	5 (5)	1.3 0.4-1.2	.678
>8	56	17 (30)	3.3 1.7-6.3	<.001	9 (16)	4.2 1.5-11.8	.006
Grading system for lymph vessel tumor emboli							
Grade 0	282	26 (9)	1		9 (3)	1	
Grade 1	115	15 (13)	1.5 0.8-2.9	.260	6 (5)	1.3 0.4-1.2	.678
Grades 2 or 3	41	16 (39)	3.1 1.6-6.4	.002	9 (22)	4.2 1.5-11.8	.006
p53 Allred score risk classes of tumor-stromal fibroblasts forming and not forming a fibrotic focus in primary invasive ductal carcinomas							
Low	336	28 (8)	1		9 (3)	1	
Inter	86	24 (28)	2.4 1.4-4.3	.003	12 (14)	3.6 1.4-9.3	.009
High	12	5 (42)	3.7 1.3-10.8	.014	3 (25)	7.0 1.4-35.8	.019

t6.1 **Table 6** Multivariate analyses for tumor recurrence and tumor-related death in patients with histologic grade 3 invasive ductal carcinoma

	Cases	Tumor recurrence			Tumor-related death		
		Cases (%)	HR, 95% CI	*P*	Cases (%)	HR, 95% CI	*P*
No. of mitotic figures in metastatic mammary carcinoma to the lymph nodes							
No	167	31 (19)	1		10 (6)	1	
<5	58	16 (28)	1		8 (14)	1	
>5	116	56 (48)	1.9 (1.2-3.1)	.007	38 (33)	3.1 (1.5-6.1)	.001
Blood vessel invasion							
Absent	280	75 (27)	1		37 (13)	1	
Present	61	28 (46)	2.1 (1.3-3.3)	.003	19 (31)	2.0 (1.1-3.7)	.017
Fibrotic focus, diameter (mm), in primary invasive ductal carcinomas							
Absent	193	51 (26)	1		24 (12)	1	
<8	69	18 (26)	0.9 (0.5-1.6)	.660	9 (13)	1.2 (0.5-2.7)	.714
>8	79	34 (43)	1.7 (1.0-2.9)	.049	23 (29)	2.0 (1.1-3.7)	.037
Grading system for lymph vessel tumor emboli							
Grade 0	205	43 (21)	1		18 (9)	1	
Grade 1	62	15 (24)	0.9 (0.5-1.6)	.649	9 (15)	1.0 (0.4-2.4)	.945
Grade 2	50	27 (54)	2.2 (1.3-3.7)	.005	14 (28)	2.1 (1.1-4.0)	.036
Grade 3	24	18 (75)	2.7 (1.4-5.4)	.004	15 (63)	3.3 (1.6-6.9)	.002
p53 Allred score risk classes of tumor-stromal fibroblasts forming and not forming a fibrotic focus in primary invasive ductal carcinomas							
Low	169	32 (19)	1		9 (5)	1	
Inter	133	49 (37)	2.0 (1.9-16.7)	.002	30 (23)	4.0 (1.9-8.6)	<.001
High	31	18 (58)	2.3 (1.2-4.5)	.014	14 (26)	4.2 (1.6-10.7)	.003

increased the hazard ratio for tumor recurrence ($P = .002$), and the presence of a nodal metastasis with a maximum dimension greater than 20 mm significantly increased the hazard ratio for tumor-related death in the multivariate analyses ($P = .032$).

4. Discussion

This study clearly indicated that the number of mitotic figures in metastatic mammary carcinoma to the lymph nodes was a very important histologic predictor of outcome for patients with invasive ductal carcinoma, independent of the nodal status or the histologic grade of the primary invasive ductal carcinoma, confirming the results of our previous study [11]. Furthermore, the number of mitotic figures in metastatic mammary carcinoma to the lymph nodes had a significantly greater outcome predictive power than the number of nodal metastases or the size of the nodal metastases in multivariate analyses performed in this study. These results strongly suggest that the biologic characteristics of metastatic mammary carcinoma to the lymph nodes are more important than the quantity of metastatic mammary carcinoma to the lymph nodes when predicting the outcome of patients with invasive ductal carcinoma.

This study also clearly demonstrated that the number of mitotic figures in metastatic mammary carcinoma to the lymph nodes is superior to the number of mitotic figures in the primary invasive ductal carcinoma for accurately predicting the outcome of patients with invasive ductal carcinoma, independent of the nodal status or the histologic grade of the primary invasive ductal carcinoma. Although the reason for this observation remains unclear, pathologists should evaluate the number of mitotic figures in metastatic mammary carcinoma to the lymph nodes but not necessarily the number of mitotic figures in the primary invasive ductal carcinoma to assess the true malignant potential of invasive ductal carcinomas accurately.

Although the number of mitotic figures is 1 factor that contributes to the histologic grade of the primary invasive ductal carcinoma and metastatic mammary carcinoma to the lymph nodes, the outcome predictive power of the number of mitotic figures in metastatic mammary carcinoma to the

lymph nodes was superior to that of the histologic grade of the primary invasive ductal carcinoma or metastatic mammary carcinoma to the lymph nodes. This finding strongly suggests that pathologists can accurately assess the true malignant potential of invasive ductal carcinomas using only the number of mitotic figures in metastatic mammary carcinoma to the lymph nodes, independent of the structural atypia or nuclear atypia observed in the tumor cells. Furthermore, the multivariate analyses in this study clearly showed the excellent outcome predictive power of the number of mitotic figures in metastatic mammary carcinoma to the lymph nodes among patients with invasive ductal carcinoma regardless of the histologic grade. Thus, the number of mitotic figures in metastatic mammary carcinoma to the lymph nodes may be a very useful histologic factor for the subclassification of patients within each histologic grade of invasive ductal carcinoma into a low- or high-risk category.

This study also clearly showed that the grading system for lymph vessel tumor emboli and the p53 Allred risk classes of tumor-stromal fibroblasts forming and not forming a fibrotic focus are significant predictors of outcome for patients with invasive ductal carcinoma, independent of the nodal status or histologic grade of the primary invasive ductal carcinoma. In addition, the presence of blood vessel invasion was a significant predictor of outcome for patients overall, for patients with nodal metastases, and for patients with histologic grade 2 invasive ductal carcinoma. The fibrotic focus diameter was also a significant predictor of outcome for patients overall and for patients with histologic grade 2 or 3 invasive ductal carcinoma. Thus, in addition to the number of mitotic figures in metastatic mammary carcinoma to the lymph nodes, the grading system for lymph vessel tumor emboli and the p53 Allred risk classes of tumor-stromal fibroblasts forming and not forming a fibrotic focus are likely to be very important predictors of outcome, whereas the presence of blood vessel invasion and the fibrotic focus diameter are likely to be of secondary importance.

In conclusion, this study clearly demonstrated the excellent outcome predictive power of the number of mitotic figures in metastatic mammary carcinoma to the lymph nodes. In the future, investigations of the factors that accelerate the proliferative activity of metastatic mammary carcinoma to the lymph nodes are likely to be very important for devising adjuvant therapies targeting such factors and for improving the prognosis of patients with invasive ductal carcinoma.

References

[1] Fisher ER, Palekar A, Rockette H, Redmond C, Fisher B. Pathologic findings from the national surgical adjuvant breast project. (Protocol No. 4) V. Significance of axillary nodular micro- and macrometastases. Cancer 1978;42:2032-8.

[2] Rosen PP, Saigo PE, Braun DW, Weathers E, Fracchia A, Kinne DW. Axillary micro- and macrometastases in breast cancer. Prognostic significance of tumor size. Ann Surg 1981;194:585-91.

[3] Fisher ER, Gregorio RM, Redmond C, Kim WS, Fisher B. Pathologic findings from the national surgical adjuvant breast project. (Protocol No. 4) The significance of extranodal extension of axillary metastases. Am J Clin Pathol 1976;65:439-45.

[4] Mignano JE, Zahurak ML, Chakaravarthy A, Piantadosi S, Dooley WC, Gage I. Significance of axillary lymph node extranodal soft tissue extension and indicators for postmastectomy irradiation. Cancer 1999;86:1258-62.

[5] Donegan WL, Stine SB, Samter TG. Implications of extracapsular nodal metastases for treatment and prognosis of breast cancer. Cancer 1993;72:778-82.

[6] Fisher B, Slack NH. Number of lymph nodes examined and the prognosis of breast carcinoma. Surg Gynecol Obstet 1970;131:79-88.

[7] Jatoi I, Hilsenbeck SG, Clark GM, Osborne CK. Significance of axillary lymph node metastasis in primary breast cancer. J Clin Oncol 1999;17:2334-40.

[8] Querzoli P, Pediriali M, Rinaldi R, et al. Axillary lymph node nanometastases are prognostic factors for disease-free survival and metastatic relapse in breast cancer patients. Clin Cancer Res 2006;12: 6696-701.

[9] de Mascarel I, MacGrogan G, Debled M, Brouste V, Mauriac L. Distinction between isolated tumor cells and micrometastases in breast cancer is it reliable and useful? Cancer 2008;112:1672-8.

[10] Andersson Y, Frisell J, Sylvan M, de Boniface J, Bergkvist L. Breast cancer survival in relation to the metastatic tumor burden in axillary lymph nodes. J Clin Oncol 2010;28:2868-73.

[11] Hasebe T, Sasaki S, Imoto S, Ochiai A. Histological characteristics of tumor in vessels and lymph nodes are significant predictors of progression of invasive ductal carcinoma of the breast: a prospective study. Hum Pathol 2004;35:298-308.

[12] Sobin LH, Gospodarowicz MK, Wittekind Ch. In: Sobin LH, Gospodarowicz MK, Wittekind Ch, editors. International Union Aganinst Cancer TNM classification of malignant tumours. 7th ed. Geneva: Wiley-Liss; 2009. p. 181-93.

[13] Bloom HJG, Richardson WW. Histological grading and prognosis in breast cancer. Br J Cancer 1957;11:359-77.

[14] Gilchrist KW, Gray R, Fowble B, et al. Tumor necrosis is a prognostic predictor for early recurrence and death in lymph node-positive breast cancer: a 10-year follow-up study of 728 eastern cooperative oncology group patients. J Clin Oncol 1993;11:1929-35.

[15] Hasebe T, Tsuda H, Hirohashi S, et al. Fibrotic focus in infiltrating ductal carcinoma of the breast: a significant histopathological prognostic parameter for predicting the long-term survival of the patients. Breast Cancer Res Treat 1998;49:195-208.

[16] Hasebe T, Sasaki S, Imoto S, et al. Prognostic significance of fibrotic focus in invasive ductal carcinoma of the breast: a prospective observational study. Mod Pathol 2002;15:502-16.

[17] Hasebe T, Yamauchi C, Iwasaki M, et al. Grading system for lymph vessel tumor emboli for prediction of the outcome of invasive ductal carcinoma of the breast. Hum Pathol 2008;39:427-36.

[18] Hasebe T, Okada N, Iwasaki M, et al. Grading system for lymph vessel tumor emboli: significant outcome predictor for invasive ductal carcinoma of the breast. Hum Pathol 2010;41:706-15.

[19] Harvey JM, Clark GM, Osborne K, et al. Estrogen receptor status by immunohistochemistry is superior to the ligand-binding assay for predicting response to adjuvant endocrine therapy in breast cancer. J Clin Oncol 1999;17:1474-81.

[20] Mohsin S, Weiss H, Havighurst T, et al. Progesterone receptor by immunohistochemistry and clinical outcome in breast cancer: a validation study. Mod Pathol 2004;17:1545-54.

[21] Allred DC, Clark GM, Elledge R, et al. Association of p53 protein expression with tumor cell proliferation rate and clinical outcome in node-negative breast cancer. J Natl Cancer Inst 1993; 85:200-6.

[22] Hasebe T, Okada N, Iwasaki M, Tamura N, et al. p53 expression in tumor stromal fibroblasts is associated with the outcome of patients with invasive ductal carcinoma of the breast. Cancer Sci 2009;100: 2101-8.
[23] Hasebe T, Iwasaki M, Akashi-Tanaka S, et al. p53 expression in tumor-stromal fibroblast forming and not forming fibrotic foci in invasive ductal carcinoma of the breast. Mod Pathol 2010;23: 662-72.
[24] Wolff AC, Hammond ME, Schwartz JN, et al. American Society of Clinical Oncology/College of American Pathologists guideline recommendations for human epidermal growth factor receptor 2 testing in breast cancer. Arch Pathol Lab Med 2007;131:18-43.

Discrepancy Between Local and Central Pathological Review of Radical Prostatectomy Specimens

Kentaro Kuroiwa,* Taizo Shiraishi, Osamu Ogawa, Michiyuki Usami, Yoshihiko Hirao and Seiji Naito for the Clinicopathological Research Group for Localized Prostate Cancer Investigators

From the Department of Urology, Graduate School of Medical Sciences, Kyushu University, Fukuoka (KK, SN), Kyoto University Graduate School of Medicine, Kyoto (OO), Osaka Medical Center for Cancer and Cardiovascular Diseases, Osaka (MU), Nara Medical University, Kashihara (YH), and Department of Pathologic Oncology, Mie University Graduate School of Medicine, Tsu (TS), Japan

Abbreviations and Acronyms

CR = central review
CRPC = Clinicopathological Research Group for Localized Prostate Cancer
ECE = extracapsular extension
GS = Gleason score
ISUP = International Society of Urological Pathology
LNI = lymph node involvement
LR = local review
PSA = prostate specific antigen
PSM = positive surgical margin
RP = radical prostatectomy
SVI = seminal vesicle invasion

Submitted for publication June 29, 2009.
Presented at annual meeting of American Urological Association, Chicago, Illinois, April 25–30, 2009.
Study received institutional review board approval.
* Correspondence: Department of Urology, Graduate School of Medical Sciences, Kyushu University, 3-1-1 Maidashi, Higashi-ku, Fukuoka 812-8582 Japan (e-mail: humeiten@hotmail.com).

See Editorial on page 850.

Purpose: Pathological assessment of radical prostatectomy specimens has not been uniform among pathologists. We investigated interobserver variability of radical prostatectomy specimen reviews between local and central pathologists.
Materials and Methods: We collated data from 50 institutions on 2,015 patients with cT1c-3 prostate cancer who underwent radical prostatectomy between 1997 and 2005. All radical prostatectomy specimens were retrospectively reevaluated by a central uropathologist. Gleason score, extracapsular extension, seminal vesicle invasion, lymph node involvement, positive surgical margin, year of diagnosis and pathology volume were recorded.
Results: The exact concordance rate of Gleason score between local and central review was 54.8%, and under grading and over grading rates at local review were 25.9% and 19.2%, respectively. Spearman's rank correlation coefficient was 0.61 for local and central radical prostatectomy Gleason score. The exact concordance rate of Gleason score 8–10 at local review was significantly lower than that of Gleason score 5–6, 3 + 4 and 4 + 3 at local review ($p = 0.011$, <0.001 and 0.006). Exact concordance rates between local and central review for extracapsular extension, seminal vesicle invasion, lymph node involvement and positive surgical margin were 82.5%, 97.6%, 99.6% and 87.5%, respectively. High volume institutions and recently diagnosed cohorts showed significantly higher exact concordance rates between local and central review for radical prostatectomy Gleason score and other pathological features (all $p < 0.001$).
Conclusions: High volume institutions and recent series show higher concordance between local and central review of radical prostatectomy pathology. However, concordance for high grade Gleason score, extracapsular extension and surgical margin status remains poor. Radical prostatectomy specimens should be reevaluated in a multi-institutional study for more accurate pathological data.

Key Words: pathology, prostatic neoplasms, prostatectomy

PATHOLOGICAL features of radical prostatectomy specimens such as Gleason score, extracapsular extension, seminal vesicle invasion, lymph node involvement and positive surgical margin are crucial observations for physicians to assess the prognosis of each patient. Various nomograms predicting PSA relapse after RP have been constructed based on these pathological features combined with preoperative PSA.[1–3] Therefore, ideally these features should be diagnosed uniformly among pathologists. However, there is concern about

0022-5347/10/1833-0952/0
THE JOURNAL OF UROLOGY®

Vol. 183, 952-957, March 2010
Printed in U.S.A.
DOI:10.1016/j.juro.2009.11.024

interobserver variability for pathological features of RP specimens, which would affect prognostic accuracy.

Interobserver variability for biopsy GS among pathologists is well documented.[4–9] Biopsy GS assigned by pathologists at an academic center has been reported as better correlated with RP GS than that by pathologists at community centers.[4,9] However, to our knowledge interobserver variability for RP GS has not been investigated in a large contemporary RP series.

There are only a few studies of interobserver variability for other pathological features of RP specimens.[10–12] It was reported that the exact concordance between local and central review of RP specimens for ECE, SVI and PSM was 57.5%, 94.0% and 69.4%, respectively, in patients with pT3/PSM.[11] On the other hand, expert uropathologists indicated good concordance when evaluating ECE (91.2%, $\kappa = 0.63$) and PSM (90.4%, $\kappa = 0.74$).[12]

We investigated the interobserver variability between local and central pathologists for RP pathological features in a large RP series of 2,015 patients. Central review for GS was based on the 2005 ISUP consensus. In addition, we analyzed the impact of the date of diagnosis and pathology volume on interobserver variability.

MATERIALS AND METHODS

Patient Population

The CRPC disease registry collates data on clinically localized prostate cancer accrued from 108 academic and community practices throughout Japan. Between 1997 and 2005 patients with clinically localized (cT1c–3) prostate cancer who underwent RP were enrolled in the CRPC registry after obtaining institutional review board approval from each center.

Of these CRPC patients pathological slides of biopsy and prostatectomy specimens were available from 50 institutions in 2,015 patients with no preoperative therapy. In all patients preoperative diagnosis was made by systemic biopsy (6 or more cores). Preoperative serum PSA was known for all patients. Clinical stage was determined by digital rectal examination and was assigned according to the 2002 American Joint Committee on Cancer staging system.

Pathological Assessment

Prostatectomy specimens from the patients were processed by a whole mount technique after formalin fixation at each institution.[13] All pathological slides of biopsy specimens were reviewed by a uropathologist (TS). All pathological slides of RP specimens were reviewed by 1 uropathologist (KK) who has reviewed more than 5,000 RP cases. GS was assigned according to the 2005 ISUP consensus, and categorized into 5 groups of 2–4, 5–6, 3 + 4, 4 + 3 and 8–10.[14] Global GS that considered the entire tumor within the prostate as 1 lesion was recorded for RP specimens since the GS of each tumor was not available in the original reports for most patients. The exact concordance rate for categorized Gleason score between original (local) and central review was investigated. Tertiary Gleason pattern in RP specimens was not reflected as primary or secondary pattern on the final RP GS.

The presence of ECE, SVI, LNI and PSM was recorded for all RP specimens. ECE level was further categorized as focal ECE and established ECE.[15] ECE was assigned as positive when tumor cells existed beyond the confines of the prostate.[16] Direct contact between tumor cells and adipose tissue was not needed to assign ECE. The presence of tumor cells at the inked margin of resection was considered a PSM. For specimens that had not been inked before formalin fixation the presence of tumor cells at the noninked margin of resection was considered a PSM. SVI was assigned as positive when tumor cells had invaded into the muscular coat of the extraprostatic seminal vesicle. The positive to negative rate for ECE, SVI, LNI and PSM was defined as No. centrally negative cases in locally positive cases/No. locally positive cases. The negative to positive rate was defined conversely.

Data from original pathological reports for RP GS, ECE, SVI, LNI and PSM were available in 1,774, 1,630, 1,639, 1,914 and 1,579 patients, respectively. All data for ECE, SVI, LNI and PSM were available in 1,526 patients. For influence of date of diagnosis we compared patients diagnosed by local pathologists in 1997 to 2003 with those diagnosed in 2004 to 2005. For pathology volume we defined high volume institutions as those contributing 100 or more patients to the CRPC registry and low volume institutions as those contributing less than 100 patients.

Statistical Analysis

Spearman's rank correlation coefficient (r) on the relationship of RP GS was generated. Simple kappa statistics were used for concordance between local and central review in ECE, SVI, PNI and PSM. The chi-square test was used for comparison of the exact concordance rate between local and central review for each pathological feature. All p values are 2-sided and $p < 0.05$ considered significant.

RESULTS

Preoperative Characteristics

Median patient age was 66 years (range 42 to 84) and median PSA was 8.5 ng/ml (range 0.5 to 85.9). A total of 1,327 patients (65.9%) had cT1c disease. For biopsy specimens the distribution of central biopsy GS 2–4, 5–6, 3 + 4, 4 + 3 and 8–10 was 0.1% (2), 33.6% (677), 27.4% (552), 19.0% (382) and 20.0% (402), respectively (table 1).

Concordance for RP GS

Table 2 shows concordance for RP GS between local and central review. Spearman's rank correlation coefficient was 0.61 for local and central RP GS. Overall exact concordance between central and local review was 54.8%, and the under grading and over grading rate in local review was 25.9% and 19.2%, respectively. When GS 3 + 4 and 4 + 3 were combined the exact concordance rate was 66.0%. All 67 cases with local review GS 2–4 were upgraded to GS

Table 1. *Preoperative clinicopathological characteristics*

No. tumor stage (%):	
T1c	1,327 (65.9)
T2a	363 (18.0)
T2b	163 (8.1)
T2c	132 (6.6)
T3	30 (1.5)
No. ng/ml PSA distribution (%):	
4.0 or Less	152 (7.5)
4.1–10.0	1,135 (56.3)
10.1–20.0	543 (26.9)
20.1 or Greater	185 (9.2)

5–6 or more by central review and 36 (53.7%) were upgraded to GS greater than 7. At local review the exact concordance rate of GS 8–10 was significantly lower than that of GS 5–6, 3 + 4 and 4 + 3 ($p = 0.011$, <0.001 and 0.006, respectively). The distribution of GS 2–4, 5–6, 3 + 4, 4 + 3 and 8–10 changed from 3.8%, 32.0%, 33.0%, 15.7% and 15.6% on local review to 0.0%, 26.0%, 40.8%, 23.3% and 9.9%, respectively, on central review.

Concordance for ECE, SVI, LNI and PSM

Concordance for ECE, SVI, LNI and PSM is shown in table 3. Positive rate for each pathological feature was similar between local and central review. Exact concordance rates (κ) between local and central review for ECE, SVI, LNI and PSM were 82.5% (0.59), 97.6% (0.82), 99.6% (0.93) and 87.5% (0.73), respectively. Exact concordance for patients with no ECE, focal ECE and established ECE by central review was 85.8% (946 of 1,102), 57.9% (121 of 209) and 85.0% (271 of 319), respectively.

Of 528 patients with positive ECE on local review 157 had negative ECE on central review (positive to negative rate 29.7%), whereas 129 of 1,102 patients with negative ECE on local review had positive ECE on central review (negative to positive rate 11.7%). For SVI, LNI and PSM the positive to negative rate was 21.5%, 3.9% and 15.6%, and the negative to positive rate was 0.9%, 0.3% and 10.9%, respectively. Of 1,526 patients the complete concordance rate for ECE, SVI, LNI and PSM was 73.5% (1,121 of 1,526).

Pathology Volume

For RP GS we identified 1,063 patients from 10 high volume institutions and 711 from 37 low volume institutions. As shown in table 4 high volume institutions had significantly higher exact concordance between local and central review for RP GS than low volume institutions (60.9% vs 45.9%, $p < 0.001$). Of 1,526 patients with all data for ECE, SVI, LNI and PSM available 962 were from 10 high volume institutions and 564 were from 34 low volume institutions. High volume institutions also had significantly higher exact concordance rates for all of these features than low volume institutions (77.1% vs 67.2%, $p < 0.001$).

Date of Diagnosis

Overall patients originally diagnosed in 2004 to 2005 had a significantly higher exact concordance rate between local and central review than those diagnosed in 1997 to 2003 for RP GS (63.1% vs 48.2%, $p < 0.001$) and all other pathological features (78.6% vs 68.1%, $p < 0.001$, table 4). This improvement in pathological concordance in more recently diagnosed patients was observed at high and low volume institutions.

DISCUSSION

Pathological features on RP specimens are important for physicians to predict the prognosis of each patient.[1,2] Adjuvant radiotherapy or hormonal therapy might be selected for patients with adverse pathological features on RP specimens such as ECE, SVI, PSM and LNI, although RP may offer long-term survival even to such patients.[17–20] However, in reality pathological assessment is not performed uniformly among pathologists and interobserver variability does exist.

For biopsy specimens of prostate cancer interobserver variability for biopsy GS has been abundantly investigated.[4–9] Recent educational efforts by the pathology community might have improved biopsy GS concordance between community hospitals and academic centers.[4] The ISUP consensus also improved GS correlation between biopsy and RP spec-

Table 2. *Concordance for radical prostatectomy Gleason score between local and central review*

	No. CR RP GS*						
RP GS (No. LR)	5–6	3 + 4	4 + 3	8–10	% Exact Concordance	% Under Grading by LR vs CR	% Over Grading by LR vs CR
2–4 (67)	31	25	8	3	0	100	0.0
5–6 (567)	318	189	48	12	56.1	43.9	0.0
3+4 (585)	99	363	112	11	62.1	21.0	16.9
4+3 (279)	10	85	163	21	58.4	7.5	34.1
8–10 (276)	3	62	82	129	46.7	0.0	53.3
Overall (1,774)	461	724	413	176	54.8	25.9	19.2

* No cases of GS 2–4 on central review.

Table 3. *Concordance between local and central review*

LR	CR Pos	CR Neg	% Exact Concordance (κ value)	% Pos LR at RP	% Pos CR at RP	p Value	% Pos to Neg	% Neg to Pos
ECE:			82.5 (0.59)	32.4	30.7	0.291	29.7	11.7
Pos	371	157						
Neg	129	973						
SVI:			97.6 (0.82)	7.4	6.6	0.373	21.5	0.9
Pos	95	26						
Neg	13	1,505						
LNI:			99.6 (0.93)	2.7	2.8	0.767	3.9	0.3
Pos	49	2						
Neg	5	1,858						
PSM:			87.5 (0.73)	34.6	36.4	0.298	15.6	10.9
Pos	461	85						
Neg	113	920						

imens.[21] On the other hand, there are only a few reports regarding interobserver variability for pathological features on RP specimens.[10–12]

Significant discordance between general pathologists and uropathologists for RP GS has been reported in limited patients.[10] However, 22% of RP specimens were not processed by whole mount technique and detailed information for pathological assessment, such as categorization of GS and concordance in each GS, was not mentioned in that study. In our study using whole mount step sections and based on central review according to the ISUP consensus, the exact concordance rate between local and central review was 54.8%, and under grading or over grading in local pathology was observed in 25.9% and 19.2%, respectively. By central review the number of patients with RP GS 2–4, 5–6 and 8–10 decreased, and the number of those with RP GS 3 + 4 and 4 + 3 increased. Local pathologists in our study assigned RP GS 2–4 in 67 (3.8%) patients, whereas none did in central review. For biopsy specimens ISUP recommends that GS 2–4 should rarely, if ever, be diagnosed.[14] Because GS 2–4 was rarely assigned in contemporary RP series from academic centers, we would emphasize that GS 2–4 should seldom be assigned even in RP specimens.[4,21]

Table 4. *Impact of pathology volume and date of diagnosis on pathological concordance*

	No. RP GS Concordance (%)	No. ECE, SVI, LNI + PSM Concordance (%)
Pathology vol:		
Low	326/711 (45.9)	379/564 (67.2)
High	647/1,063 (60.9)	742/962 (77.1)
p Value	<0.001	<0.001
Date of diagnosis:		
1997–2003	473/981 (48.2)	511/750 (68.1)
2004–2005	500/793 (63.1)	610/776 (78.6)
p Value	<0.001	<0.001
Low/1997–2003	195/480 (40.6)	209/303 (62.8)
Low/2004–2005	131/231 (56.7)	170/231 (73.6)
p Value	<0.001	0.007
High/1997–2003	278/501 (55.5)	302/417 (72.4)
High/2004–2005	369/562 (65.7)	440/545 (80.7)
p Value	0.001	0.002

We also found poorer concordance between local and central review for high grade GS (8–10) compared with other GS (5–6, 3 + 4, 4 + 3). Of cases assigned as GS 8–10 by local review 53.3% were downgraded to 5–6, 3 + 4 or 4 + 3 by central review. This poor concordance in high grade GS may contribute to lower concordance between local and central review in our study compared with the previous study on biopsy GS that included only 32 high grade GS cases at local review (66.1% vs 76.5%).[4]

Unlike biopsy specimens with limited sample size, the discrepancy of GS in RP specimens among pathologists may reflect differences of interpretation itself for each Gleason pattern. We believe that this discrepancy can be effectively improved by educational effort as has been observed with biopsy specimens.[4] Indeed recently diagnosed RP specimens in our study showed higher GS concordance than those diagnosed earlier regardless of pathology volume. This improvement may be due to educational efforts by the pathology community as well as personal efforts of each pathologist even before the ISUP consensus. The ISUP consensus may result in further improvement for RP GS concordance between local and central review.

van der Kwast et al studied 552 RP specimens from multiple institutions, and observed poor concordance between local and central review for ECE (57.5%) and PSM (69.4%), and good concordance for SVI (94.0%).[11] Conversely good concordance was observed among 12 expert uropathologists for ECE (91.2%, $\kappa = 0.63$) and PSM (90.4%, $\kappa = 0.74$) in a small selected RP series.[12] We found excellent exact concordance for SVI (97.6%, $\kappa = 0.82$) and LNI (99.6%, $\kappa = 0.93$). The exact concordance rate in our study between local and central review for ECE (82.5%, $\kappa = 0.59$) and PSM (87.5%, $\kappa = 0.73$) was

better than that in a previous study comparing local and central pathologists (κ = 0.33 and 0.45).[11]

Although we should not simply compare κ values between studies because of the difference of data set, there may be some reasons for this difference. Since our study included more recently diagnosed patients, the effect of date of diagnosis as shown in our study may contribute to this higher concordance. Another contributing factor might be the fact that our patients underwent RP for cT1c–3 disease rather than more advanced disease (pT3 or PSM). The high κ values for ECE and PSM in our study as in a study with expert uropathologists (κ = 0.60 and 0.74) do not necessary mean that concordance in local and central pathologists is equivalent to that among expert uropathologists, because the study with expert uropathologists seems to include more difficult cases than our study.[12]

We found low concordance in patients with focal ECE at central review compared with those with established ECE (57.9% vs 85.0%). Since the prostate lacks a true histological capsule, and the boundaries between prostate and surrounding tissue are sometimes poorly defined especially with apical and anterior lesions, interobserver variability for ECE exists even among expert uropathologists.[12,22] ECE criteria for apical or anterior site remain to be established. Most cases in which definite judgment of ECE is difficult to make may have focal ECE.

We assigned PSM only when tumor cells touched the margin of resection. Most patients who were negative for PSM at local review and positive at central review were considered close to the margin by the central pathologist.

We also investigated the positive to negative and negative to positive rates for ECE, SVI, LNI and PSM. Although there were no differences regarding overall positive rates between local and central pathologists for each pathological feature, we found high positive to negative and negative to positive rates except for LNI. For SVI the positive to negative rate was 21.5% despite excellent overall concordance (97.6%).

It was previously reported that concordance between local and central review for ECE, SVI and PSM was essentially the same regardless of pathology volume.[11] We found that for GS and other pathological features local review at high volume institutions had higher concordance with central review than at low volume institutions. In high volume institutions there may be more communication between pathologists and urologists regarding pathological specimens, and pathologists may pay more attention to assessment for RP specimens. As in RP GS more recently diagnosed RP specimens in our study showed higher concordance for pathological features other than GS than those diagnosed at an earlier date in low and high volume institutions.

CONCLUSIONS

Although concordance between local and central pathologists was excellent for SVI and LNI, that for high grade GS, ECE and PSM was less satisfactory. This discrepancy may affect the outcomes of each pathological feature. High volume institutions showed higher concordance than low volume institutions. Although the concordance has recently improved, more educational and/or personal effort is warranted. For more precise pathological assessment we recommend central review for a study with RP specimens from multiple institutions.

REFERENCES

1. Kattan MW, Wheeler TM and Scardino PT: Postoperative nomogram for disease recurrence after radical prostatectomy for prostate cancer. J Clin Oncol 1999; **17:** 1499.
2. Stephenson AJ, Scardino PT, Eastham JA et al: Postoperative nomogram predicting the 10-year probability of prostate cancer recurrence after radical prostatectomy. J Clin Oncol 2005; **23:** 7005.
3. Walz J, Chun FK, Klein EA et al: Nomogram predicting the probability of early recurrence after radical prostatectomy for prostate cancer. J Urol 2009; **181:** 601.
4. Fine SW and Epstein JI: A contemporary study correlating prostate needle biopsy and radical prostatectomy Gleason score. J Urol 2008; **179:** 1335.
5. King CR: Patterns of prostate cancer biopsy grading: trends and clinical implications. Int J Cancer 2000; **90:** 305.
6. Lattouf JB and Saad F: Gleason score on biopsy: is it reliable for predicting the final grade on pathology? BJU Int 2002; **90:** 694.
7. Paulson DF: Impact of radical prostatectomy in the management of clinically localized disease. J Urol 1994; **152:** 1826.
8. San Francisco IF, DeWolf WC, Rosen S et al: Extended prostate needle biopsy improves concordance of Gleason grading between prostate needle biopsy and radical prostatectomy. J Urol 2003; **169:** 136.
9. Steinberg DM, Sauvageot J, Piantadosi S et al: Correlation of prostate needle biopsy and radical prostatectomy Gleason grade in academic and community settings. Am J Surg Pathol 1997; **21:** 566.
10. Ekici S, Ayhan A, Erkan I et al: The role of the pathologist in the evaluation of radical prostatectomy specimens. Scand J Urol Nephrol 2003; **37:** 387.
11. van der Kwast TH, Collette L, Van Poppel H et al: Impact of pathology review of stage and margin status of radical prostatectomy specimens (EORTC trial 22911). Virchows Arch 2006; **449:** 428.
12. Evans AJ, Henry PC, van der Kwast TH et al: Interobserver variability between expert urologic pathologists for extraprostatic extension and surgical margin status in radical prostatectomy specimens. Am J Surg Pathol 2008; **32:** 1503.

13. Montironi R, van der Kwast T, Boccon-Gibod L et al: Handling and pathology reporting of radical prostatectomy specimens. Eur Urol 2003; **44:** 626.

14. Epstein JI, Allsbrook WC Jr, Amin MB et al: The 2005 International Society of Urological Pathology (ISUP) Consensus Conference on Gleason Grading of Prostatic Carcinoma. Am J Surg Pathol 2005; **29:** 1228.

15. Wheeler TM, Dillioglugil O, Kattan MW et al: Clinical and pathological significance of the level and extent of capsular invasion in clinical stage T1-2 prostate cancer. Hum Pathol 1998; **29:** 856.

16. Srigley JR, Amin MB, Epstein JI et al: Updated protocol for the examination of specimens from patients with carcinomas of the prostate gland. Arch Pathol Lab Med 2006; **130:** 936.

17. Bolla M, van Poppel H, Collette L et al: Postoperative radiotherapy after radical prostatectomy: a randomised controlled trial (EORTC trial 22911). Lancet 2005; **366:** 572.

18. Messing EM, Manola J, Yao J et al: Immediate versus deferred androgen deprivation treatment in patients with node-positive prostate cancer after radical prostatectomy and pelvic lymphadenectomy. Lancet Oncol 2006; **7:** 472.

19. Thompson IM Jr, Tangen CM, Paradelo J et al: Adjuvant radiotherapy for pathologically advanced prostate cancer: a randomized clinical trial. JAMA 2006; **296:** 2329.

20. Boorjian SA, Thompson RH, Siddiqui S et al: Long-term outcome after radical prostatectomy for patients with lymph node positive prostate cancer in the prostate specific antigen era. J Urol 2007; **178:** 864.

21. Helpap B and Egevad L: The significance of modified Gleason grading of prostatic carcinoma in biopsy and radical prostatectomy specimens. Virchows Arch 2006; **449:** 622.

22. Ayala AG, Ro JY, Babaian R et al: The prostatic capsule: does it exist? Its importance in the staging and treatment of prostatic carcinoma. Am J Surg Pathol 1989; **13:** 21.

Comparison of evaluations of hormone receptors in breast carcinoma by image-analysis using three automated immunohistochemical stainings

KOJI ARIHIRO, MIYO ODA, KATSUNARI OGAWA, KENSHI TOMINAGA, YOSHIE KANEKO, TOMOMI SHIMIZU, SHIHO OHNISHI, MEGUMI ODA, YUKI KURITA, YUKO TAIRA, MASAYOSHI FUJII and MAIKO TANAKA

Department of Anatomical Pathology, Hiroshima University Hospital, Hiroshima 734-8551, Japan

Received June 22, 2010; Accepted August 6, 2010

DOI: 10.3892/etm.2010.142

Abstract. The aim of this study was to compare the results of immunohistochemistry (IHC) assays evaluated by human examiners with the results evaluated by computerized image analysis, and to compare the computerized image analysis results among three automated IHC assays, namely the BioGenex, Dako and Ventana assays. All slides were semiquantitatively evaluated according to the Allred score and J-score by human examiners. The images were analyzed using MacSCOPE version 2.6 for Macintosh according to the H-score and the percentage of positive-stained nuclei per area of carcinoma cells (PP) irrespective of the intensity of the stained nuclei. The H-score for the estrogen receptor (ER) was significantly correlated with the Allred score ($P<0.0001$) and the PP for the ER was significantly correlated with the J-score ($P<0.0001$), suggesting that the image analysis used in the present study is a useful method for the evaluation of ER status. Several discrepancies were identified between the Allred score and H-score and between the PP and J-score due to the positive-stained cytoplasm area of carcinoma cells and/or the positive-stained nuclei area of non-carcinoma cells, including benign epithelial cells, lymphocytes and stromal cells. Accordingly, advances in the algorithm of the digitized analyzing system is necessary.

Introduction

Although a refined assessment of hormone receptors in breast carcinoma is necessary to select therapeutic agents, endocrine responsiveness has recently been defined as the presence of any detectable estrogen receptor (ER) according to the recommendations and thresholds for the post-operative adjuvant systemic therapy of early breast cancer proposed by the St. Gallen International Expert Consensus meeting in 2009 (1). In other words, the previous three categories of endocrine responsiveness using 1 and 10% cut-off values have been simplified, so that endocrine therapy is considered when any ER-positive cells are noted in the tumor. For the evaluation of hormone receptor (HR) status, it is recommended that the percentage of HR-positive cells be indicated on pathology reports rather than merely using scores. In particular, positivity for HRs of 50% or more of tumor cells is viewed as indicating highly endocrine-responsive tumors, suggesting that the HR must be reliably and accurately measured.

As to the immunohistochemistry (IHC) methods for the detection and quantification of the ER and progesterone receptor (PgR), the authors compared evaluations for HRs in breast carcinoma using two manual and three automated IHC assays, and showed intermethod variability indicated by multi-rater κ-values for the ER and PgR (ER, $\kappa=0.34$; PgR, $\kappa=0.45$) (2). In addition, to assess low levels of HR expression, the HR was evaluated by real-time monitoring polymerase chain reaction (RT-PCR) using complementary DNA produced by reverse transcription of the messenger RNA of each breast carcinoma. Although we showed an excellent correlation between RT-PCR results and those of the IHC method, there were some discrepancies between the results of RT-PCR and IHC due to the overestimation of HR-positive lymphocytes and mesenchymal cells in tumor stroma, among other factors (3).

To provide a standardized semi-quantitative measurement of the HR for IHC specimens, computerized image analysis has been employed since the late 1980s (4). These attempts were performed using various systems or software, including Cell Analysis System's CAS 100 (4), BIOCOM500 (5), CAS 200 (6), Image cytometry (7), Adobe Photoshop (8,9), computer-supported analysis (10), SpectraCube™ (11), Chroma Vision Automated Cellular Imaging System (ACIS) (12-14), WinROOF (15), QCA (16) and VISUAL C^{++} (17). In particular, automated image analysis technology, including AQUA (18), Ariol (14,19) and MatLab7 using digital image capturing (20), has recently been developed. Although it is emphasized that computerized image analysis has improved quantification, reproducibility and interobserver variability for the HR evaluation of breast carcinoma (4-20), the process

Correspondence to: Dr Koji Arihiro, Department of Anatomical Pathology, Hiroshima University Hospital, 1-2-3 Kasumi, Minami-ku, Hiroshima 734-8551, Japan
E-mail: arihiro@hiroshima-u.ac.jp

Key words: estrogen receptor, immunohistochemistry, automated staining, image analysis

of image analysis is known to be more time consuming and labor intensive than assessment by the human eye.

In Japan, there are three automated IHC methods approved by the Japanese Ministry of Health, Labor and Welfare to assess HR status in order to determine the suitability of endocrine treatment: automated IHC staining by Dako (Dako Corp., Glostrup, Denmark), BioGenex Corp. (San Ramon, CA, USA) and Ventana Medical Systems (Tucson, AZ, USA), each of which uses a different method for retrieving antigens and different types of antibodies or detection reagents. To date, no studies have directly compared these IHC computerized image analysis methods.

The aim of the present study was to assess the intermethod variability of these three IHC assays using image analysis. An additional aim was to find an optimal condition for image analysis that may be proposed as a reliable assay for ER determination.

Materials and methods

Samples. Fifty consecutive cases of invasive ductal carcinoma of the breast that had been surgically resected in 2004 and 2005 were selected from the files of the Department of Anatomical Pathology, Hiroshima University Hospital. H&E-stained slides of each case were reviewed, and the presence of invasive carcinoma and adjacent non-neoplastic breast tissue was confirmed in all cases. The histological type of each tumor was invasive ductal carcinoma, not otherwise specified.

IHC assay for ER. From formalin-fixed, paraffin-embedded tissues, five 4-μm sections were serially cut and mounted on pre-coated slides. IHC assays were carried out as described in previous reports (2,3).

For IHC by the BioGenex system using an automated i6000 immunostainer (BioGenex Corp.), anti-ER mouse monoclonal antibody (mAb), ER88 (BioGenex Corp.) was used. Immunoperoxidase staining was performed according to the manufacturer's instructions (BioGenex Corp.).

For IHC by the Dako system using the Dako Autostainer™, anti-ER mAb, 1D5 (Dako Corp.) was used. Immunoperoxidase staining was performed according to the manufacturer's instructions (Dako Corp.).

For IHC by the Ventana system using the Ventana HX System BenchMark™ (Ventana Medical Systems), anti-ER mAb, 6F11 (Ventana Medical Systems) was used. All procedures were performed automatically in BenchMark™. Immunoperoxidase staining was performed according to the manufacturer's instructions (Ventana Medical Systems). Diaminobenzidine (DAB) was used as a chromogen substrate in all specimens. The sections were counterstained with hematoxylin.

Scoring system for human examiners. First, the presence or absence of staining of the nuclei of non-neoplastic ducts and acini in adjacent tissue was observed and was used as an internal control. The site for evaluation was not limited to the invasive area, but incorporated the entire lesion. Two scoring systems were used to evaluate the IHC findings, the Allred score (21) and J-score (2,3,22). The J-score comprises proportional values irrespective of the intensity of stained nuclei, and the proportion of cells stained in each specimen was recorded as 0, none; 1, <1%; 2, 1-10%; 3, ≥10%, as advocated and employed as the cut-off points in previous reports (23,24).

All study specimens were scored by two different examiners (K.A. and M.O.) masked to the patient characteristics.

Computer-assisted digital analysis. Ten images were selected by pathologists and captured from each section at x200 magnification through a Hamamatsu C5810 color chilled 3CCD camera (Hamamatsu, Japan). The captured images were saved as JPEG images on the image analysis computer. When contamination by normal tissue was present, the pathologist exchanged it manually for another field, including the tumor area. The images were analyzed using MacSCOPE version 2.6 (Mitani Corp., Tokyo, Japan) for Macintosh. Despite the area selection, a certain minimum contamination of the automatic measurement by host cells is inevitable when stromal and normal cells are intimately associated with tumor cells. To distinguish non-carcinoma cell elements from the non-immunostained carcinoma cell nuclei on the digitized image, nuclei with small areas (<25 μm^2 gross area) and spindle features (>0.5 oval rate) were regarded as lymphocyte nuclei or nucleic debris and stromal cell nuclei, respectively, and were eliminated. Nuclei that stained brown or blue were extracted automatically using two distinct macroinstructions composed chiefly of algorithms for color extraction based on red-green-blue (RGB) parameters divided into 256 arbitrary units. To create the digitized image-based procedures for determining ER status, the threshold value of the RGB parameters of each intensity score (IS) was established as: 0, negative; 1, weak nuclear staining, faintly perceptible at high power magnification; 2, intermediate stained nuclei; 3, nuclei displaying strong staining that had the appearance of an ink dot at low power magnification, according to the Allred score (Fig. 1).

Scoring system. Two scoring systems were used to evaluate the ER findings using computer-assisted analysis: the H-score method (15,25) and the percentage of area of stained nuclei of carcinoma cells (PP) in 10 images, irrespective of the intensity of stained nuclei. The H-score was calculated by summing 3x the percentage of total nuclei area showing IS3, 2x the percentage of total nuclei area showing IS2 and 1x the percentage of total nuclei area showing IS1, ranging from 0 to 300.

Statistical analysis. The Spearman's rank correlation test was used for correlation analysis between the H-score and the total score (TS) of the Allred score and between the PP and J-score.

Results

Relationship between Allred score and H-score for ER. A comparison of the distribution of the TS of Allred scores determined by the human examiners and that of H-scores calculated by image-analysis software for ER by the three staining methods is shown in Fig. 2. The H-score values for the same group of tumors increased monotonically as the TS increased, although there was considerable variability among tumors with the same TS. The Spearman's rank correlation coefficient between the two methods ranged from 0.572 to 0.889 ($P<0.0001$). The cut-off values of H-scores for the ER

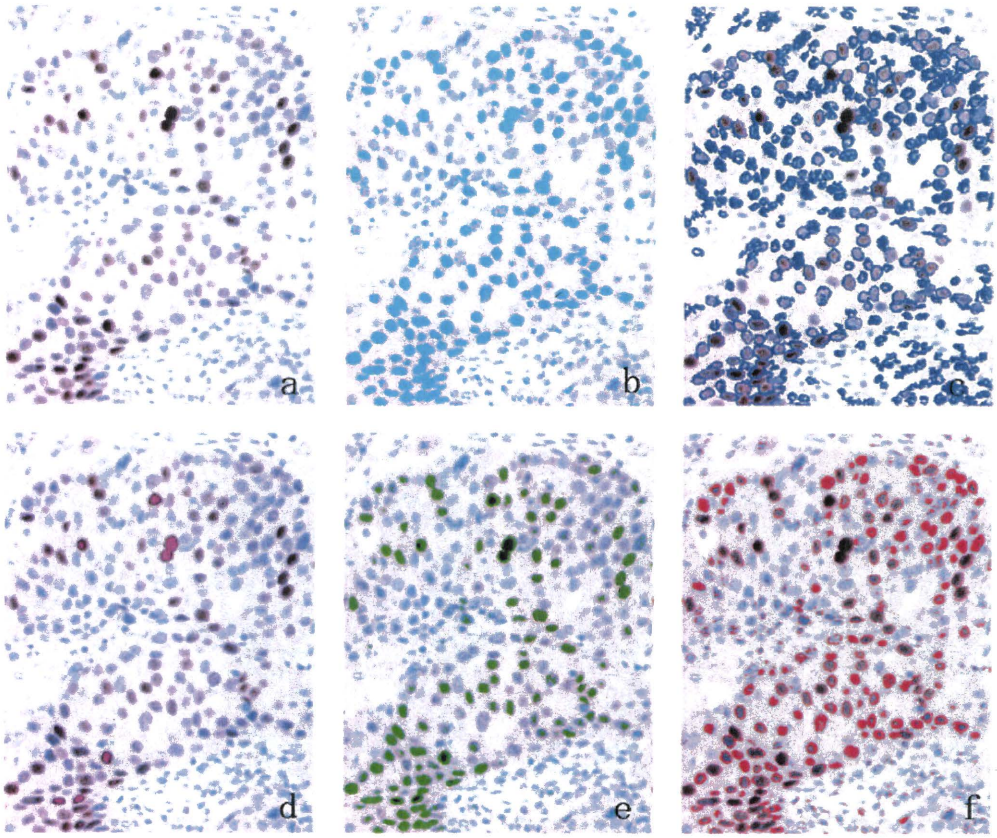

Figure 1. Immunohistochemistry of ER and the images analyzed by MACScope. (a) Nuclei of carcinoma cells show various intensities of the ER. (b) All positive-stained nuclei of carcinoma cells are shown in light blue; 3,994.4 μm^2. (c) All negative-stained nuclei of carcinoma cells are shown in blue; 5,409.3 μm^2. (d) Strongly stained nuclei of carcinoma cells are shown in pink; 92.6 μm^2. (e) Intermediately stained nuclei of carcinoma cells are shown in green; 1,728.9 μm^2. (f) Weakly stained nuclei of carcinoma cells are shown in red; 2,173 μm^2.

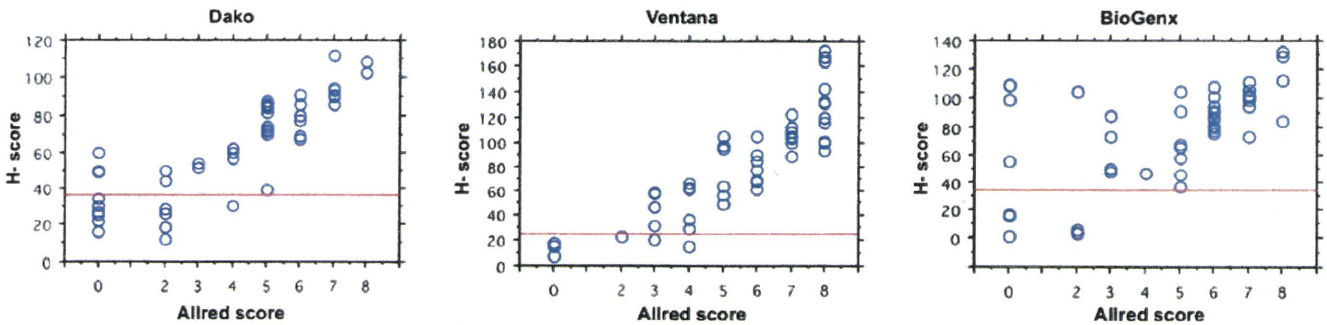

Figure 2. Scattergram of H-score with Allred score for the ER. The H-score was significantly correlated to the Allred total score of IHC using the Dako, Ventana and BioGenex assays (Spearman's rank correlation test, P<0.0001). The cut-off values in the Dako, Ventana and BioGenex assays were 36, 24 and 34 (red line), respectively.

determined by the Dako, Ventana and BioGenex assays were regarded as 36, 24 and 34 according to the Allred score, respectively. The concordance rates at these cut-off values were the highest of each IHC assay, and 88, 98 and 90% among the IHC results generated by the Dako, Ventana and BioGenex assays, respectively.

Relationship between J-score and PP for ER. A comparison of the distribution of J-scores scored by the human examiners and that of the percentage of positive cells calculated by image-analyzing software for ER by the three staining methods is shown in Fig. 3. The Spearman's rank correlation coefficient between the two methods ranged from 0.495 to 0.914. The cut-off values of the PP for ER determined by the Dako, Ventana and BioGenex assays were regarded as 37, 36 and 38 according to the J-score, respectively. The concordance rates at these cut-off values were the highest of each IHC assay, and 90, 92 and 84% among the IHC results generated by the Dako, Ventana and BioGenex assays, respectively.

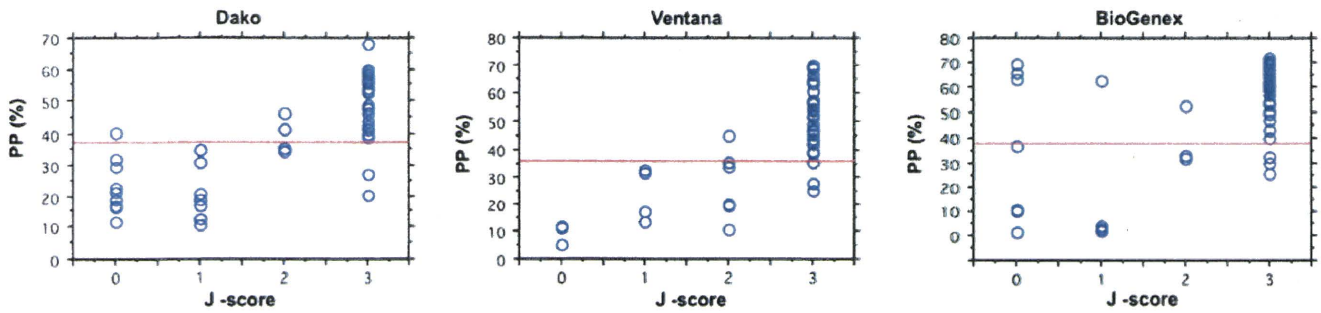

Figure 3. Scattergram of PP with J-score for the ER. The PP is significantly correlated to the J-score for the ER using the Dako, Ventana and BioGenex assays (Spearman's rank correlation test, P<0.0001). The cutoff values in the Dako, Ventana and BioGenex assays were 37, 36 and 38 (red line), respectively.

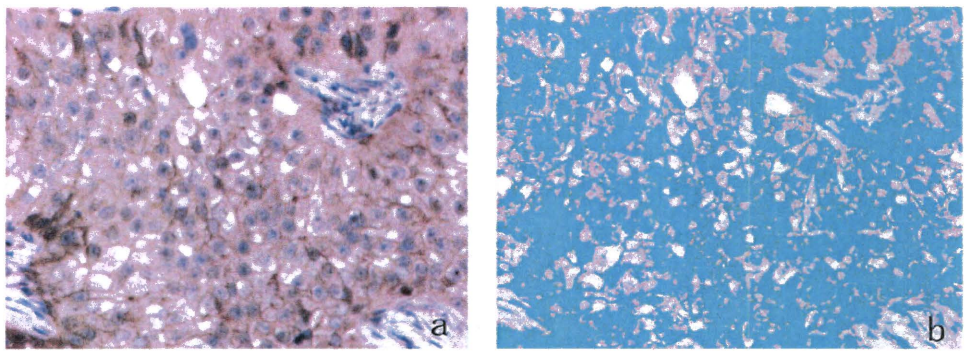

Figure 4. Immunohistochemistry of the ER and the images analyzed by MACScope. (a) ER positivity was noted not only in the nuclei, but also in the membrane and/or cytoplasm of carcinoma cells. (b) All positive-stained areas of carcinoma cells are shown in light blue. ER status was overestimated.

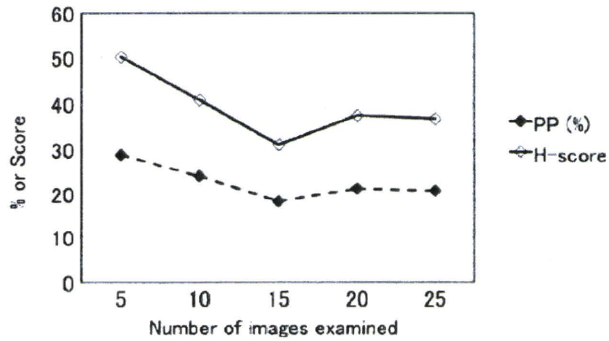

Figure 5. Correlation between numbers examined by computerized image analysis, H-score and the PP of ER in a representative case. The H-score and PP show a plateau in more than 20 images examined.

Procedures. Approximately 4 min were required to capture 10 images from each specimen and to process these image analyses per case. The individual results of 50 cases of breast carcinoma in the present study were transferred to another software program for calculation.

Discussion

In the present study, quantification of ER using image-analyzing software was performed and compared to semi-quantitative assessment by histopathologists. A high degree of correlation between the two was revealed. Although various studies concerning computerized image analysis have been conducted (4-25), it is difficult to compare the various systems directly, due to the absence of reliable and universal gold standards.

With regard to a cut-off value for ER evaluation by computerized image analysis, 10% of positive cells (9,16,20), the H-score (15) and AQUA scores calculated by the average signal intensity divided by compartment area (18) were used in previous reports. Although in the present study the Allred score determined by human examiners was compared to the H-score calculated by the computer and the Allred/H-score conversion table was shown in a previous report (26), it was difficult to translate one scoring system to the other system, precisely since the two systems are not strictly equivalent. Accordingly, the final assessment of the clinical usefulness of these various systems, cut-off values and estimation methods is thought to depend on the correlation with biological behavior and responsiveness to hormone therapy.

In the present study, there were some discrepancies between human observation and computerized image analysis for IHC. For the cases showing negativity on human observation and positivity on computerized image analysis for ER, the software used detected ER expression in the lymphocytes and mesenchymal cells. Since ER expression of infiltrating lymphocytes and mesenchymal cells in tumor stroma has been reported previously (3,27), a condition was set to eliminate non-carcinoma cells showing positivity, although it was not possible to completely eliminate the ER expression of lymphocytes or mesenchymal cells.

Additionally, in the present study, ER expression in the cytoplasm or plasma membrane of carcinoma cells was noted in 3.5, 2 and 25% of examined cases using the Dako, Ventana and BioGenex assays, respectively (Fig. 4). In a previous study, the extranuclear expression of HR in breast carcinoma cells was reported in 9.5% of examined cases (28). Accordingly, the software used in the present study may have overestimated the positivity of ER in carcinoma cells, as it could not discriminate between ER expression in the nuclei and that in the cytoplasm or plasma membrane of carcinoma cells. Accordingly, it is necessary to use softwave with improved function that derives ER expression only from the nuclei of carcinoma cells.

Regarding the time required to perform computerized image analysis, in general, the process of image analysis is more time consuming and labor intensive than visual scoring from a glass slide. Although in a previous report the processing time for 100 images from 20 cases by WinROOF was reportedly approximately 60 min, excluding the time required to capture the images (15), there have been few reports discussing the time necessary to capture and process the images by software. In the present study, the capture and processing time for 10 images per case was approximately 4 min. In comparison to the study using WinROOF, the process of image analysis in the present study was less time consuming and labour intensive due to the improved function of the computer and software.

With regard to the number of images captured for digitized analysis, there have been various numbers of images used ranging from the single best field (16,17), three fields (8), four fields (14), five fields (5,15,29), eight fields (9) and ten fields (6,10). In the present study, ten fields were selected and captured for image analysis, similar to previous studies which used the maximal numbers of images (6,10). Although twenty fields was regarded as sufficient for digitized image analysis on the basis of a preliminary study on the relationship between the number of images digitally analyzed and H-score or the percentage of stained nuclei area (Fig. 5), the optimal number of images for digital analysis should be considered, taking into account the time required for the procedure. Recently, a fully automatic digitized analyzing system for the total fields of specimens was developed using digital images captured by the Aperio ScanScope XT Slide Scanner and algorithm by MatLab 7 (20). This system reportedly identifies only tumor nuclei and automatically excludes non-tumor structures, including stromal components and lymphocytes. In particular, it is entirely unsupervised and does not require any *a priori* data. Irrespective of the adjustment of various thresholds and cut-off values to detect various cells exhibiting particular sizes and shapes, to date, it has been difficult for a digitized analyzing system to discriminate between benign and malignant cells with complete accuracy. Accordingly, advances in the algorithm of digitized analyzing systems are necessary.

As for image analysis of the RGB system, in general, a composite color signal is built up from combinations of basic color values produced by the mosaic arrangement of three color filters (red, green and blue) on the surface of the imager. In this way, each color image is recorded as a superimposition of 3 images with a photometric resolution of 255 linear values: a red, a blue and a green one, reflecting the slide transmission into these three types of wavelengths (5). However, even when an RGB imaging system functions perfectly, there are intrinsic limitations to its ability to distinguish between similar chromogens and to isolate the optical signal from each chromogen. Thus, each color signal is quantitatively and separately measured (30). In the present study, DAB was used as a chromogen substrate, and the choice of chromogen and counterstain is known to affect both the visual and quantitative results. Accordingly, the appropriate chromogen substrate and counterstain dye suitable for image analysis must be selected.

References

1. Goldhirsch A, Ingle JN, Gelber RD, Coates AS, Thurlimann B and Senn HJ: Thresholds for therapies: highlights of the St Gallen International Expert Consensus on the primary therapy of early breast cancer 2009. Ann Oncol 20: 1319-1329, 2009.
2. Arihiro K, Umemura S, Kurosumi M, *et al*: Comparison of evaluations for hormone receptors in breast carcinoma using two manual and three automated immunohistochemical assays. Am J Clin Pathol 127: 356-365, 2007.
3. Oda M, Arihiro K, Kataoka T, Osaki A, Asahara T and Ohdan H: Comparison of immunohistochemical assays and reverse transcription real-time polymerase chain reaction for analyzing status of hormone receptors in human breast carcinoma. Pathol Int 60: 305-315, 2010.
4. Bacus S, Flowers JL, Press MF, Bacus JW and McCarty KS Jr: The evaluation of estrogen receptor in primary breast carcinoma by computer-assisted image analysis. Am J Clin Pathol 90: 233-239, 1988.
5. Rostagno P, Birtwisle I, Ettore F, *et al*: Immunohistochemical determination of nuclear antigens by colour image analysis: application for labelling index, estrogen and progesterone receptor status in breast cancer. Anal Cell Pathol 7: 275-287, 1994.
6. Layfield LJ, Saria EA, Conlon DH and Kerns BJ: Estrogen and progesterone receptor status determined by the Ventana ES 320 automated immunohistochemical stainer and the CAS 200 image analyzer in 236 early-stage breast carcinomas: prognostic significance. J Surg Oncol 61: 177-184, 1996.
7. Cohen C: Image cytometric analysis in pathology. Hum Pathol 27: 482-493, 1996.
8. Lehr HA, Mankoff DA, Corwin D, Santeusanio G and Gown AM: Application of photoshop-based image analysis to quantification of hormone receptor expression in breast cancer. J Histochem Cytochem 45: 1559-1565, 1997.
9. Bejar J, Sabo E, Misselevich I, Eldar S and Boss JH: Comparative study of computer-assisted image analysis and light-microscopically determined estrogen receptor status of breast carcinomas. Arch Pathol Lab Med 122: 346-352, 1998.
10. Mofidi R, Walsh R, Ridgway PF, *et al*: Objective measurement of breast cancer oestrogen receptor status through digital image analysis. Eur J Surg Oncol 29: 20-24, 2003.
11. Rothmann C, Barshack I, Gil A, Goldberg I, Kopolovic J and Malik Z: Potential use of spectral image analysis for the quantitative evaluation of estrogen receptors in breast cancer. Histol Histopathol 15: 1051-1057, 2000.
12. Vesoulis Z, Rajappannair L, Define L, Beach J, Schnell B and Myers S: Quantitative image analysis of estrogen receptors in breast fine needle aspiration biopsies. Anal Quant Cytol Histol 26: 323-330, 2004.
13. Fisher ER, Anderson S, Dean S, *et al*: Solving the dilemma of the immunohistochemical and other methods used for scoring estrogen receptor and progesterone receptor in patients with invasive breast carcinoma. Cancer 103: 164-173, 2005.
14. Gokhale S, Rosen D, Sneige N, *et al*: Assessment of two automated imaging systems in evaluating estrogen receptor status in breast carcinoma. Appl Immunohistochem Mol Morphol 15: 451-455, 2007.
15. Hatanaka Y, Hashizume K, Nitta K, Kato T, Itoh I and Tani Y: Cytometrical image analysis for immunohistochemical hormone receptor status in breast carcinomas. Pathol Int 53: 693-699, 2003.
16. Diaz LK, Sahin A and Sneige N: Interobserver agreement for estrogen receptor immunohistochemical analysis in breast cancer: a comparison of manual and computer-assisted scoring methods. Ann Diagn Pathol 8: 23-27, 2004.